NANO LETTERS

2004
Vol. 4, No. 6
1029−1034

A Localized Surface Plasmon Resonance Biosensor: First Steps toward an Assay for Alzheimer's Disease

Amanda J. Haes,[†] W. Paige Hall,[†,‡] Lei Chang,[‡] William L. Klein,*[,‡] and Richard P. Van Duyne*[,†]

Department of Chemistry, Northwestern University, 2145 Sheridan Road, Evanston, Illinois 60208-3113, and Department of Neurobiology and Physiology, Northwestern University, 2205 Tech Drive, Evanston, Illinois 60208

Received March 1, 2004; Revised Manuscript Received April 14, 2004

ABSTRACT

The localized surface plasmon resonance (LSPR) nanosensor based on the optical properties of Ag nanotriangles is shown to aid in the understanding of the interaction between amyloid β-derived diffusible ligands (ADDL) and the anti-ADDL antibody, molecules possibly involved in the development of Alzheimer's disease. By varying the concentration of anti-ADDL antibody, a surface confined binding constant of 3.0×10^7 M^{-1} for the interaction of ADDLs and anti-ADDLs was measured. Influences of Cr, the nanoparticle adhesion layer, will be shown to be the limiting factor in the sensitivity of this assay. This is the first nonmodel application of the LSPR nanosensor.

Greater understandings of nanoscience and nanoscale phenomena are vital for the development of devices based on nanotechnology. Relevant to this work, the potential to develop highly sensitive and specific sensors for biological targets motivates a portion of the research in this field. Previously, we have presented results based on the nanoscale limit of surface plasmon resonance sensors. This novel, nanoscale development, termed the localized surface plasmon resonance (LSPR) nanosensor, is a refractive index based sensing device that relies on the extraordinary optical properties of noble (Ag, Au, Cu) metal nanoparticles.[1−5] The LSPR, which refers to the ability of the conduction electrons in the nanoparticle to oscillate collectively,[6] induces electromagnetic fields surrounding the nanoparticle which determine the sensing volume in which refractive index based sensing can occur.[5,7] Because the conduction electrons oscillate collectively to only specific wavelengths of light, nanoparticles exhibit selective photon absorption, which can easily be monitored using ultraviolet−visible (UV−vis) spectroscopy. It is well established that the maximum extinction wavelength, λ_{max}, of the LSPR is dependent upon the composition, size, shape, and interparticle spacing of the nanoparticles as well as the dielectric properties of their local environment (i.e., substrate, solvent, and surface-confined molecules).[5,7−9]

In previous work, we have shown that LSPR nanosensors are useful in detecting biological molecules.[2,4,10] The extinction maximum of Ag nanoparticles fabricated using nanosphere lithography (NSL) produced consistent wavelength shifts to the red with increasing density and thickness of adsorbate layers. Biological sensing was demonstrated for large proteins and antibodies. The magnitude of the wavelength shift response was determined by the size and packing density of the molecules on the nanoparticle surface and the limit of detection of the system were determined by the surface-confined binding constant between the capture ligand on the surface and the target molecule in solution. Because the systems revealed no nonspecific binding,[2] the entire response could be attributed to the specific interactions between the molecules of choice. Since these initial studies, optimization of the LSPR nanosensor has been realized by adjusting the size and shape of the nanoparticles.[5,7] These studies, which occurred in combination with theoretical calculations, revealed areas of heightened electromagnetic field strength located at the corners of the nanoparticles[7] as well as an overall tunable sensing volume that was determined by the average induced electromagnetic fields that

* Corresponding authors. R. P. Van Duyne: vanduyne@chem.northwestern.edu, Telephone: (847) 491-3516, Fax: (847) 491-7713. W. L. Klein: wklein@northwestern.edu, Telephone: (847) 491-5510, Fax: (847) 491-5211.
[†] Department of Chemistry.
[‡] Department of Neurobiology and Physiology.

10.1021/nl049670j CCC: $27.50
Published on Web 05/04/2004

surround the nanoparticles.[5] These findings encouraged us to apply our knowledge about nanoparticle-based sensors to a biologically relevant system for the possible diagnosis of Alzheimer's disease.

Alzheimer's disease is the leading cause of dementia in people over age 65 and affects an estimated 4 million Americans.[11] At present, there is no consensus regarding disease mechanism. However, a comprehensive review of current data has concluded that early stages of the disease are likely to be caused by the synaptic impact of soluble oligomeric assemblies of amyloid-β (Aβ).[12] Aβ is a 42-amino acid peptide that was first discovered as the monomeric subunit of the large insoluble amyloid fibrils of Alzheimer's disease plaques. In the past several years, it has been found that, in addition to plaques, Aβ will also self-assemble into small soluble oligomers, termed ADDLs, (amyloid-derived diffusible ligands) and that ADDLs experimentally will cause neurological dysfunctions relevant to memory.[13−15] ADDLs, moreover, are present and significantly elevated in autopsied brain samples from humans with Alzheimer's disease.[16] Association of ADDLs with disease mechanisms and brain pathology suggests that a sensitive means to detect ADDLs in body fluid detection could provide a definitive molecular basis for the clinical laboratory diagnosis of Alzheimer's disease. At present, no such laboratory test exists. Also, because ADDLs are potent immunogens,[17] the detection of ADDL-specific antibodies might provide a related approach to diagnostics. Ultrasensitive methods for ADDLs or anti-ADDL antibody detection potentially could emerge from LSPR nanosensor technology, providing an opportunity to develop the first clinical lab diagnostic for Alzheimer's disease. The work presented here utilizes LSPR spectroscopy to demonstrate the sensitivity of ADDL-functionalized nanoparticles to anti-ADDL antibodies. Influences of Cr, the nanoparticle adhesion layer, will be shown to be the limiting factor in the sensitivity of this sensor.

Nanosphere lithography (NSL) was used to create monodisperse, surface-confined Ag nanotriangles.[2,5] Polystyrene nanospheres ($\sim$2.2 μL, diameter = 390 nm $\pm$ 19.5 nm, Duke Scientific) were drop-coated onto piranha-cleaned and base-treated glass substrates[2] (Fisher) and were allowed to dry, forming a hexagonal close-packed monolayer of spheres, which served as a deposition mask. The samples were mounted into a Consolidated Vacuum Corporation vapor deposition chamber. A Leybold Inficon XTM/2 quartz crystal microbalance was used to monitor the thickness of the metal being deposited. A thin Cr adhesion layer (0.4 nm, R. D. Mathis) was first deposited onto the nanosphere masks to promote nanoparticle adhesion. Next, 25 nm of Ag (D. F. Goldsmith) was evaporated onto the samples. Following metal deposition, the samples were sonicated for 3−5 min in ethanol (Pharmco) to remove the polystyrene nanosphere mask, creating individual platforms of Cr that promote the adhesion of the Ag nanoparticles to the glass substrate. Atomic force microscope (AFM) images were collected using a Digital Instruments Nanoscope IV microscope and Nanoscope IIIa controller operating in tapping mode. Resulting AFM linescan analysis reveals that the bare nanoparticles are triangular, have $\sim$90 nm perpendicular bisectors, and are $\sim$28−29 nm tall (0.4 nm Cr, 25 nm Ag, 2.5−3.5 nm increase in height from slight nanoparticle restructuring[2]).

The LSPR spectrum of the nanoparticles is slightly broadened and dampened from the Cr adhesion layer (less than 10% change from a spectrum collected from nanoparticles without Cr); however, the increased nanoparticle adhesion allows for harsh flow and chemical conditions and was therefore used for these experiments. Figure 1A shows a cartoon representation of the nanoparticle structure and functionalization. A self-assembled monolayer (SAM) of 1:3 11-mercaptoundecanoic acid (11-MUA, Aldrich))/1-octanethiol (1-OT, Aldrich) was formed onto the surface by incubation in an ethanolic solution for 24 h. After thorough rinsing, 1-ethyl-3-[3-dimethyl-aminopropyl]carbodiimide hydrochloride (EDC, Pierce), a zero length coupling agent, was then used to covalently link ADDLs to the surface-confined carboxyl groups over a 1 h period. Given the efficiency of this interaction[4] and from AFM analysis, a full monolayer of ADDLs is estimated for each nanoparticle. The ADDLs were prepared following a protocol from Lambert.[13] Finally, varying the concentration of rabbit polyclonal anti-ADDL IgG antibody (prepared according to Lambert[17]) and exposing the solution to the samples for 30 min completed the assay. All biological solutions were prepared in 10 mM phosphate buffered saline (PBS, Sigma), and samples were rinsed thoroughly with 10 mM PBS and 20 mM PBS (Sigma).

The extinction maximum, λ_{max}, of each sample was monitored and recorded using a UV−vis spectrometer before, during, and after each incubation step (SAM, ADDL, and anti-ADDL). Macroscale UV−vis extinction measurements were collected using an Ocean Optics (Dunedin, FL) SD2000 fiber optically coupled spectrometer with a CCD detector. All spectra in this study are macroscopic measurements performed in standard transmission geometry with unpolarized light. The probe diameter was approximately 2 mm. A home-built flow cell[1,10] was used to control the external environment of the Ag nanoparticle substrates. A three-way valve was connected to the cell to allow the nanoparticle sample to be exposed to buffer, biological solutions, or nitrogen in a controlled manner. The extinction maximum of each spectrum was located by calculating its first derivative. By convention, a shift toward the red end of the spectrum is denoted as a positive (+) value while a shift toward the blue end is assigned a negative (−) value. These wavelength shifts are a more reliable indication of physical and chemical changes at the nanoparticle surface than are changes in peak intensity. Although the absolute value of the extinction maximum varied from sample to sample, it is known that this does not affect the relative response shifts of the LSPR sensor.[2,4] Such variations are a result of small differences in dielectric environment due to the adsorption of a water layer as well as slight dissimilarities in nanoparticle roughness features, and do not affect the sensitivity of the biosensor. For this reason, only the relative wavelength shift, $\Delta\lambda_{max}$, was used to monitor binding of the analytes.

By functionalizing the Ag nanoparticles with a 3:1 1 mM OT/1 mM 11-MUA SAM layer, the stability of the samples

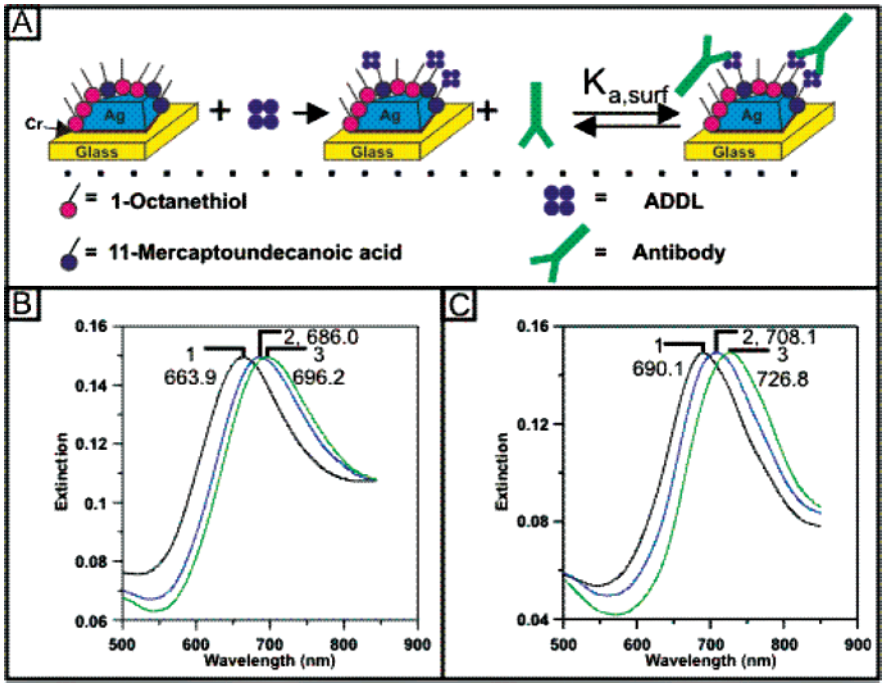

Figure 1. Design of the LSPR biosensor for anti-ADDL detection. (A) Surface chemistry of the Ag nanoparticle sensor. Surface-confined Ag nanoparticles are synthesized using NSL. Nanoparticle adhesion to the glass substrate is promoted using a 0.4 nm Cr layer. The nanoparticles are incubated in a 3:1 1-OT/11-MUA solution to form a SAM. Next, the samples are incubated in 100 mM EDC/100 nM ADDL solution. Finally, incubating the ADDL-coated nanoparticles to varying concentrations of antibody completes an anti-ADDL immunoassay. (B) LSPR spectra for each step of the preparation of the Ag nanobiosensor at a low concentration of anti-ADDL antibody. Ag nanoparticles after modification with (B-1) 1 mM 3:1 1-OT/11-MUA, $\lambda_{max} = 663.9$ nm, (B-2) 100 nM ADDL, $\lambda_{max} = 686.0$ nm, and (B-3) 50 nM anti-ADDL, $\lambda_{max} = 696.2$ nm. All spectra were collected in a N_2 environment. (C) LSPR spectra for each step of the preparation of the Ag nanobiosensor at a high concentration of anti-ADDL. Ag nanoparticles after modification with (C-1) 1 mM 3:1 1-OT/11-MUA, $\lambda_{max} = 690.1$ nm, (C-2) 100 nM ADDL, $\lambda_{max} = 708.1$ nm, and (C-3) 400 nM anti-ADDL, $\lambda_{max} = 726.8$ nm. All spectra were collected in a N_2 environment.

is greatly increased and consistent red shifts are produced upon incubation in given concentrations of both ADDLs and anti-ADDLs. Because it is hypothesized that the presence of anti-ADDLs prohibits the development of Alzheimer's disease, the assay explored here is designed to detect that antibody. Given the size of the ADDL (4.5*N kDa, N = 3−24) and anti-ADDL (150 kDa) molecules, it was hypothesized that at full coverage ADDLs may give smaller up to equivalent LSPR shifts in comparison to anti-ADDLs. Additionally, the magnitude of the LSPR shift is larger for molecules closer to the Ag surface rather than farther away from the nanoparticle surface.[5] This effect will magnify the LSPR shift induced by the ADDLs in comparison to the anti-ADDLs.

After a 24 h incubation in SAM, a representative LSPR extinction wavelength of the Ag nanoparticles is measured to be 663.9 nm (Figure 1B-1). Samples are then incubated for 1 h in 100 mM EDC/100 nM ADDL to ensure that the amide bond between the amine groups in the ADDLs and the carboxyl groups on the surface had been formed. The LSPR wavelength shift due to this binding event was measured to be +22.1 nm, resulting in a LSPR extinction wavelength of 686.0 nm (Figure 1B-2). The Ag nanoparticle biosensor is now ready to detect the specific binding of anti-ADDL. Incubation in 50 nM anti-ADDL for 30 min results in a LSPR wavelength shift of + 10.2 nm, giving a λ_{max} of 696.2 nm (Figure 1B-3). The results of this experiment are dramatically different if the concentration of anti-ADDL is increased to 400 nM. At this high concentration, the LSPR wavelength shifts +18.7 nm from 708.1 to 726.8 nm (Figure 1C) from the binding of anti-ADDLs to the ADDL functionalized nanoparticle surface.

Next, a response curve was constructed by measuring the LSPR wavelength shifts after exposure of the ADDL-functionalized surface to concentrations of anti-ADDL between 100 pM and 1 μM (Figure 2). Each data point resulted from the analysis of a different sample. The line in the figure is not a fit to the data but is a theoretical model that can be described by the following equation:[4]

$$\Delta R = \Delta R_{max}\left[\frac{K_{a,surf}[\text{anti-ADDL}]}{1 + K_{a,surf}[\text{anti-ADDL}]}\right] \qquad (1)$$

where $\Delta R = \Delta\lambda_{max}$, LSPR λ_{max} shift for a given concentration, ΔR_{max} is the maximum LSPR response measured at high concentrations, $K_{a,surf}$ is the surface-confined thermodynamic affinity constant, and [anti-ADDL] is the concentration of the anti-ADDL solution. To fit the data in Figure 2 to our model, the two lowest concentrations were excluded during this analysis.

As seen in previous work, this binding curve reveals important characteristics that describe the binding of ADDLs to anti-ADDL antibodies. First, the saturation response and

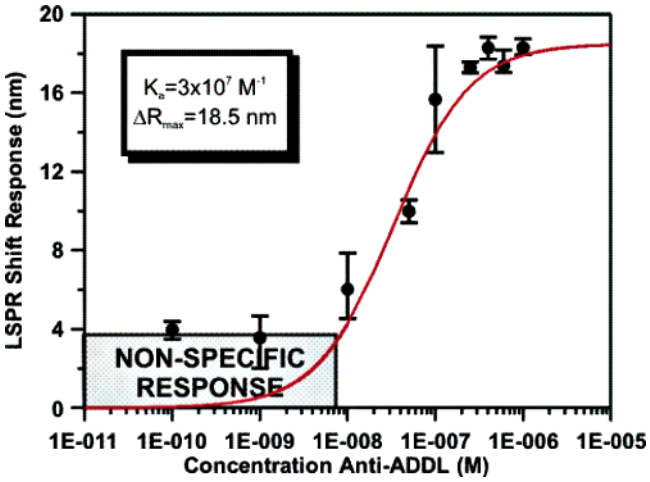

Figure 2. LSPR shift, ΔR or $\Delta\lambda_{max}$ versus [anti-ADDL antibody] response curve for the binding of anti-ADDL antibody to an ADDL-functionalized Ag nanobiosensor. All measurements were collected in a N_2 environment. The solid line is the calculated value of ΔR using eq 1.

saturation anti-ADDL concentration can be determined. Fits to the data indicate that the saturation response of the nanobiosensor is 18.5 nm and that saturation begins around 100 nM anti-ADDL. A more important characteristic determined by the binding curve is a surface confined binding constant of 3.0×10^7 M^{-1} for the interaction of ADDL and anti-ADDL. This analysis is the first determination of the ADDL/anti-ADDL binding constant and is consistent within the general range of antigen/antibody interactions.[18] In our previous studies, the limit of detection of the system was dictated by the binding constant of the molecules being studied.[2−4] This approach cannot be taken here. As seen in Figure 2, as the concentration of anti-ADDL approaches our predicted limit of detection, the wavelength shift result does not minimize to zero. Instead, the average wavelength shift minimizes to ∼4 nm. This unexpected behavior forced us to analyze the source of this unexpected, nonzero response.

In an attempt to understand the +4 nm wavelength shift response revealed at low concentrations in the anti-ADDL assay, several nonspecific binding experiments have been performed. SAM-functionalized nanoparticles are incubated in 100 nM anti-ADDL with no EDC coupling agent. If anti-ADDL molecules were binding selectively only to surface-bound ADDLs (as in Figure 2), the wavelength shift response, $\Delta\lambda_{max}$, should have been at or near 0 nm. When anti-ADDLs are exposed to a SAM-coated nanoparticle, however, results reveal an average $\Delta\lambda_{max}$= 31.9 nm shift (Figure 3A). This outcome was startling when it was compared to our previous studies of nonspecifically bound antibodies to SAM-functionalized nanoparticles which revealed a zero wavelength shift.[2] To better understand this large nonspecific response, AFM was used to examine the changes in the structures of the nanoparticles before and after exposure to the anti-ADDL solution in Figure 3A. AFM analysis of SAM-coated nanoparticles (Figure 3B) reveals a small amount of nonspecific interactions on the sample. Additional AFM images confirmed an increase in the amount of random material on the samples after incubation in anti-

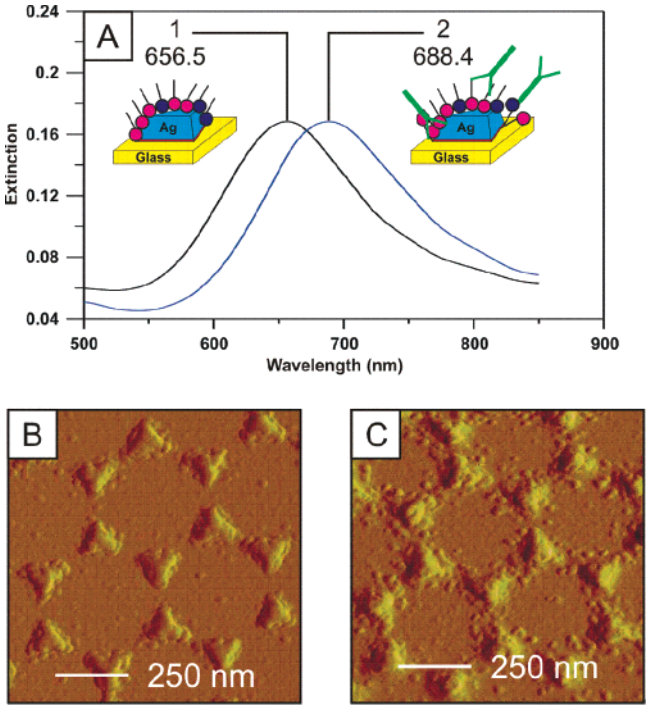

Figure 3. (A) LSPR spectra illustrating the nonspecific binding of the anti-ADDL antibody to a Ag nanobiosensor with no covalently linked ADDL. (A-1) Ag nanoparticles after modification with 1 mM 1:3 11-MUA/1-OT, λ_{max} = 656.5 nm. (A-2) Ag nanoparticles modified with 100 nM anti-ADDL, λ_{max} = 688.4 nm. All extinction measurements were collected in a N_2 environment. (B) AFM image of Ag nanoparticles functionalized with a SAM (corresponds to 3A-1 spectrum). (C) AFM image of Ag nanoparticles modified with 100 nM anti-ADDL (corresponds to 3A-2 spectrum).

ADDL (Figure 3C) (not in the presence of EDC). This study indicates that nonspecific interactions between the nanoparticles and the anti-ADDL molecules are occurring.

To more precisely analyze this issue, representative AFM images and AFM linescans from samples (30+ nanoparticles) coated with SAM (Figure 4A), anti-ADDL with no EDC (Figure 4B), and anti-ADDL specifically coupled to the surface with EDC (Figure 4C) were collected. The SAM-coated nanoparticles had average heights of 34.8 nm and average widths of 130.8 nm. As seen in Figures 4B and 4C, linescan analysis revealed small features on the sample with heights of ∼8−10 nm, roughly corresponding to the size of anti-ADDL molecules. Additionally, while only a slight increase in nanoparticle height is observed, large ∼10 nm steps at the bases of the nanoparticles can be clearly seen in the samples incubated in anti-ADDL solution (in the absence of EDC) (Figure 4B). These steps are not visible in Figure 4C. This indicates that the majority of nonspecific interactions are occurring at the base of the nanoparticles. This finding is emphasized when anti-ADDL molecules are linked to the surface specifically with EDC. As shown in Figure 4C, the linescan analyses of these resulting nanoparticles have no step edges (as seen in Figure 4B) and have an average height and width increase between 6 and 10 nm, which corresponds to the dimensions of a monolayer of antibody.

Earlier AFM and optical studies found little to no nonspecific binding evidence for the LSPR nanobiosensor.[2,4]

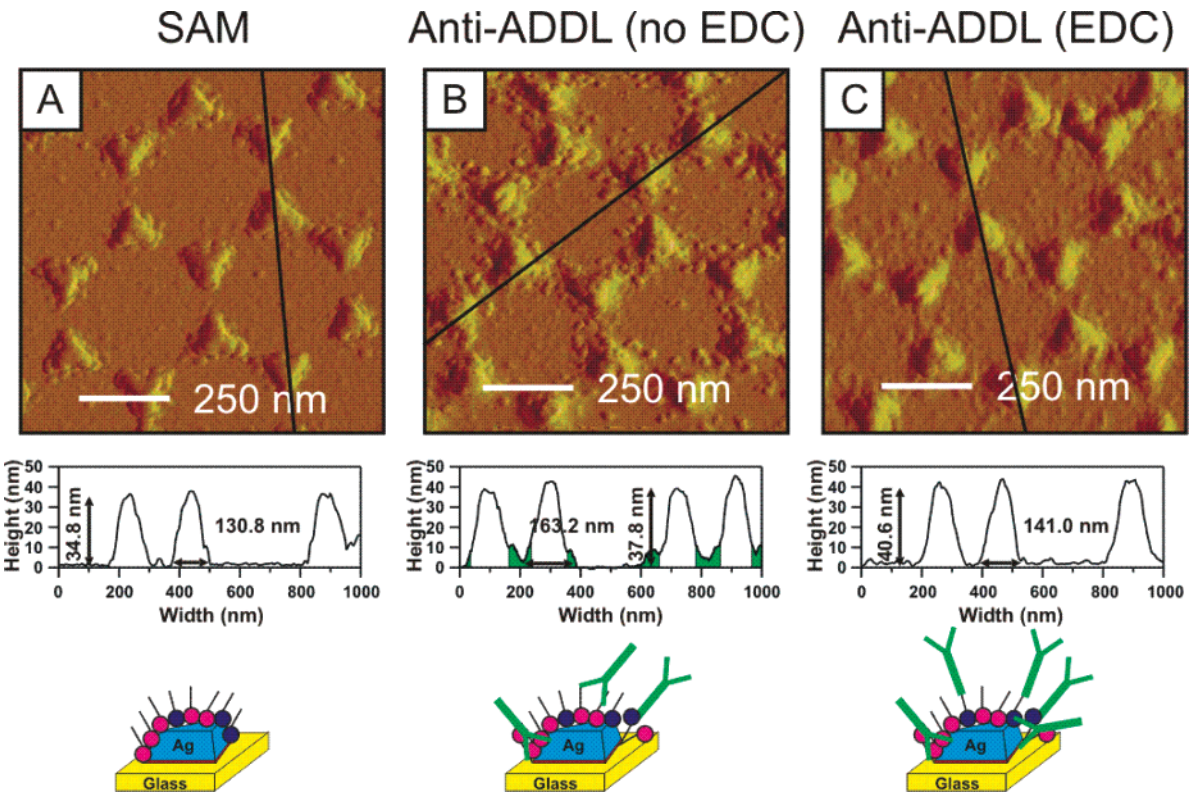

Figure 4. A tapping mode AFM and line scan analysis of the nonspecific binding of anti-ADDL to the SAM-coated Ag nanoparticle biosensor. (A) Ag nanoparticles after modification with 3:1 1-OT/11-MUA (average height = 34.8 ± 3.15 nm, average width = 130.8 ± 1.85 nm). (B) Ag nanoparticles (with SAM layer) after to 100 nM anti-ADDL solution (in the absence of EDC) (average height = 37.8 ± 1.68 nm, average width = 163.2 ± 10.2 nm). (C) A fresh Ag nanoparticle sample (with SAM layer) after modification with the direct linkage of a 100 nM anti-ADDL solution (in the presence of EDC) (average height = 40.6±2.46 nm, average width = 141.0 ± 6.11 nm).

This suggests that the Cr adhesion layer that was used in this study but not in our previous studies is interfering with the biosensor selectivity. While the detail of the nonspecific interaction is not understood, our working hypothesis is that Cr has a higher binding affinity for COOH than SH groups in alkanethiols.[19] Jung et al. showed that Cr preferentially binds to carboxyl groups, leaving the thiol available to form disulfide bonds with cysteines in the anti-ADDL molecules, increasing the nonspecific interactions at the Cr-containing portion of the nanoparticles. Previous experiments have revealed "hot-spots" on the triangular Ag nanoparticles at the corners and bases of the structures.[5,7] Because the Cr is located in an area with high electromagnetic field strength, the nonspecific interactions induced by this layer are amplified.

To analyze whether the Cr-induced nonspecific binding could be reduced, *n*-propyl trimethoxysilane (PTMS, Alpha Aesar) was used to passivate the Cr layer prior to SAM functionalization. The silane groups in the PTMS bind strongly to Cr but not to Ag, and the methyl groups passivate the surface from further fouling. In these studies, immediately following nanosphere removal, the samples were incubated in a 1 mM PTMS solution (ethanol) for varying times and then incubated in the SAM (3:1 1-OT/11-MUA) solution for 24 h. Nonspecific interactions were monitored by exposing the SAM functionalized nanoparticles to a 100 nM anti-ADDL solution (no EDC coupling agent) for 1 h. This technique dramatically decreases the degree of nonspecific binding induced by anti-ADDLs on a SAM-coated surface. Silane incubation times were varied from 0 to 72 h, and the resulting shift in λ_{max} decreased from 31.9 to 7 nm (Figure 5). Currently, the silane passivation approach is being optimized in order to retain the adhesive properties of Cr between glass and Ag as well as to reduce the level of nonspecific interactions induced by Cr.

In conclusion, the two principal discoveries reported here are as follows: (1) the nanobiosensor based on monitoring the localized surface plasmon resonance (LSPR) spectrum of Ag nanoparticles can be used to monitor the interaction between ADDLs and anti-ADDLs, molecules possibly implicated in Alzheimer's disease; and (2) a Cr adhesion layer limits the detection capabilities of the Ag nanoparticle biosensor by initiating nonspecific interactions at the bases of the nanoparticles. ADDL-functionalized Ag nanoparticles were shown to display high selectivity to elevated concentrations of anti-ADDLs. When the concentration of anti-ADDLs was decreased to ~10 nM, the LSPR shift response was primarily influenced by nonspecific interactions of the antibody with the Cr adhesion layer. This surprising result when coupled with AFM analysis, suggests that while Cr is useful for the adhesion of surface-confined nanoparticle studies, the level of nonspecific interaction reduces its practicality for sensor uses. Because Cr is often used as an adhesive layer for nanosensors, experimentalists should investigate if eliminating or replacing this layer could reduce nonspecific results. Steps to passivate the Cr adhesion layer

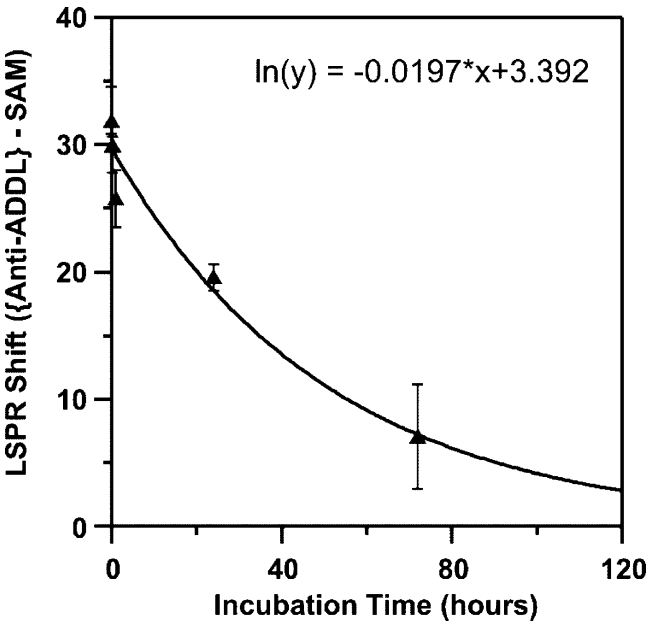

Figure 5. Exposing the samples to a 1 mM PTMS solution for 0−72 (t = 0, 0.25, 1, 24, and 72) hours passivated the Cr adhesion layer of the Ag nanoparticles. The sample was then incubated in a 3:1 1-OT/11-MUA solution for 24 h. The sample was rinsed and the LSPR spectrum was collected. Next, the sample was exposed to a 100 nM anti-ADDL solution (in the absence of EDC). Following complete rinsing, the LSPR spectrum of the sample was collected. The difference between the extinction maxima of the two spectra was compared and plotted versus PTMS incubation time. An exponential decay best fits the data: $\ln(y) = -0.0197x + 3.392$ ($R^2 = 0.9844$).

with PTMS decreased the level of nonspecific interactions but did not eliminate this undesirable result completely. Currently, other adhesion promoters and other substrates are being tested to address this issue.

Looking into the future, we expect this approach to have important implications for the understanding of Alzheimer's disease. By reducing the level of nonspecific binding, an anti-ADDL assay can be completed and may aid in the understanding of the mechanism of Alzheimer's disease. The development of an accurate diagnostic test for Alzheimer's disease is crucial and will help millions to obtain timely and appropriate treatment for their symptoms. With further improvements in both selectivity and sensitivity, the LSPR biosensor has the potential to become an accurate and economical alternative to traditional clinical assays.

Acknowledgment. The authors gratefully acknowledge financial support from the Nanoscale Science and Engineering Initiative of the National Science Foundation under NSF Award EEC-0118025. Any opinions, findings, and conclusions or recommendations expressed in this material are those of the authors and do not necessarily reflect those of the National Science Foundation. A.H. acknowledges the American Chemical Society, Division of Analytical Chemistry sponsored by Dupont for fellowship support. W.H. thanks the Nanoscale Science and Engineering Center at Northwestern University, Research Experience for Undergraduates program that is funded under NSF Award EEC-0118025.

References

(1) Malinsky, M. D.; Kelly, K. L.; Schatz, G. C.; Van Duyne, R. P. *J. Am. Chem. Soc.* **2001**, *123*, 1471.
(2) Haes, A. J.; Van Duyne, R. P. *J. Am. Chem. Soc.* **2002**, *124*, 10596.
(3) Haes, A. J.; Van Duyne, R. P. *Laser Focus World* **2003**, *39*, 153.
(4) Riboh, J. C.; Haes, A. J.; McFarland, A. D.; Yonzon, C. R.; Van Duyne, R. P. *J. Phys. Chem. B* **2003**, *107*, 1772.
(5) Haes, A. J.; Zou, S.; Schatz, G. C.; Van Duyne, R. P. *J. Phys. Chem. B* **2004**, *108*, 109.
(6) Jensen, T. R.; Kelly, K. L.; Lazarides, A.; Schatz, G. C. *J. Cluster Sci.* **1999**, *10*, 295.
(7) Haes, A. J.; Zou, S.; Schatz, G. C.; Van Duyne, R. P. *J. Phys. Chem. B* **2004**, in press.
(8) Jensen, T. R.; Malinsky, M. D.; Haynes, C. L.; Van Duyne, R. P. *J. Phys. Chem. B* **2000**, *104*, 10549.
(9) Haynes, C. L.; Van Duyne, R. P. *J. Phys. Chem. B* **2001**, *105*, 5599.
(10) Van Duyne, R. P.; Haes, A. J.; McFarland, A. D. *SPIE* **2003**, *5223*, 197.
(11) Facts About Alzheimer's Disease (www.alz.org); Alzheimer's Disease and Related Disorders Association, Inc., 2004.
(12) Selkoe, D. J.; Hardy, J. **2002**, *298*, 963.
(13) Lambert, M. P.; Barlow, A. K.; Chromy, B. A.; Edwards, C.; Freed, R.; Liosatos, M.; Morgan, T. E.; Rozovsky, I.; Trommer, B.; Viola, K. L.; Wals, P.; Zhang, C.; Finch, C. E.; Krafft, G. A.; Klein, W. L. *Proc. Natl. Acad. Sci. U.S.A.* **1998**, *95*, 6448.
(14) Walsh, D. M.; Klyubin, I.; Fadeeva, J. V.; Cullen, W. K.; Anwyl, R.; Wolfe, M. S.; Rowan, M. J.; Selkoe, D. J. **2002**, *416*, 535.
(15) Chromy, B. A.; Nowak, R. J.; Lambert, M. P.; Viola, K. L.; Chang, L.; Velasco, P. T.; Jones, B. W.; Fernandez, S. J.; Lacor, P. N.; Horowitz, P.; Finch, C. E.; Krafft, G. A.; Klein, W. L. **2003**, *42*, 12749.
(16) Gong, Y.; Chang, L.; Viola, K. L.; Lacor, P. N.; Lambert, M. P.; Finch, C. E.; Krafft, G. A.; Klein, W. L. *Proc. Natl. Acad. Sci. U.S.A.* **2003**, *100*, 10417.
(17) Lambert, M. P.; Viola, K. L.; Chromy, B. A.; Chang, L.; Morgan, T. E.; Yu, J. X.; Venton, D. L.; Krafft, G. A.; Finch, C. E.; Klein, W. L. *J. Neurochem.* **2001**, *79*, 595.
(18) *Immunoassay*; Academic Press: San Diego, CA, 1996.
(19) Jung, D. R.; Czanderna, A. W. *J. Vac. Sci. Technol. A* **1995**, *13*, 1337.

NL049670J